ARTICLES
https://doi.org/10.1038/s41558-020-0889-7

nature climate change

Climate velocity in inland standing waters

R. Iestyn Woolway[1,2] ✉ and Stephen C. Maberly[3]

Inland standing waters are particularly vulnerable to increasing water temperature. Here, using a high-resolution numerical model, we find that the velocity of climate change in the surface of inland standing waters globally was 3.5 ± 2.3 km per decade from 1861 to 2005, which is similar to, or lower than, rates of active dispersal of some motile species. However, from 2006 to 2099, the velocity of climate change will increase to 8.7 ± 5.5 km per decade under a low-emission pathway such as Representative Concentration Pathway (RCP) 2.6 or 57.0 ± 17.0 km per decade under a high-emission pathway such as RCP 8.5, meaning that the thermal habitat in inland standing waters will move faster than the ability of some species to disperse to cooler areas. The fragmented distribution of standing waters in a landscape will restrict redistribution, even for species with high dispersal ability, so that the negative consequences of rapid warming for freshwater species are likely to be much greater than in terrestrial and marine realms.

Inland standing waters hold a large majority of the Earth's liquid surface fresh water, support important biodiversity and provide key ecosystem services to people around the world[1]. Yet, standing waters are highly vulnerable to climate change. Some of the most pervasive and concerning consequences of climate change for standing waters are the direct and indirect effects of rising water temperature[2]. This temperature increase can influence physical structure, rates of processes and species composition[3,4], and in turn temperature can strongly influence the distribution and abundance of freshwater species across the globe[5]. However, within a lake or reservoir, temperature varies seasonally[6] and horizontally[7], and often vertically in those that are deep enough to stratify[8,9]. As standing waters warm over time, aquatic communities may have to disperse to track thermally suitable habitats[10]. A critical step in the understanding of climate change impacts on aquatic ecosystems is therefore to describe the speed at which their thermal environment is changing, often referred to as the velocity of climate change, that is, the distance at which isotherms shift over time[11]. The velocity of climate change has been studied extensively in marine and terrestrial ecosystems[12,13] but has not yet been investigated in standing waters globally, despite the vulnerability of freshwater species to direct and indirect thermal alterations associated with warming[14].

The velocity of climate change (km per decade) is calculated as the quotient of the long-term temperature trend (°C per decade) to the two-dimensional spatial gradient in temperature (°C km^{-1}). Here we calculated the distribution of the historical velocity of climate change in the surface of inland standing waters worldwide using surface temperatures from a new state-of-the-art global re-analysis from the European Centre for Medium-Range Weather Forecasts (ECMWF), ERA5, on a 0.25° × 0.25° grid (see Methods). Inland water temperature within ERA5 is simulated via the Freshwater Lake (FLake) model, which is embedded as a tile in the Tiled ECMWF Scheme for Surface Exchanges over Land incorporating land surface hydrology (HTESSEL). The FLake model has been extensively validated here (Extended Data Fig. 1) and in simulations of the surface temperature of inland waters globally, and has been used to quantify worldwide aspects of inland water thermal dynamics such as seasonal cycles[6], the onset of summer stratification[7] and mixing dynamics[3].

Our study demonstrates that, over a period of 40 years (1979–2018), the annual surface temperature of inland standing waters has increased in 99% of the surface grid cells analyzed, although there were substantial regional variations in magnitude (Fig. 1a). Worldwide, the median rate of warming in inland standing waters was 0.13 °C per decade (Fig. 1a). Our computed trends are similar to those calculated in previous studies which have demonstrated that the vast majority of lakes worldwide are warming[2], despite differences in the seasonal extent of the data (all year versus summer) or the range of years analysed. Across inland standing waters, the median spatial gradient in temperature was 0.009 °C km^{-1} (Fig. 1b), and it was greater in regions with large elevation gradients, such as the European Alps (Extended Data Figs. 2 and 3). When the rate of warming is combined with the spatial gradient in temperature, the resulting median velocity of climate change across standing waters worldwide was 13.94 km per decade during 1979–2018 (Fig. 1c). As a result of higher increases in surface temperatures and lower spatial gradients, the velocity of climate change is greater at mid- to high latitude (Fig. 1d) and in regions with low gradients in elevation (Extended Data Figs. 2 and 4).

We compared the velocity of climate change in inland standing waters from 1979 to 2018 with those calculated for marine and terrestrial ecosystems[11,12] by applying the same climate velocity algorithm to surface air temperatures over land and sea surface temperatures, both of which are available from ERA5. We find that the velocity of climate change in inland standing waters was comparable to that calculated for surface air temperatures over land (13.76 km per decade), despite the median rate of warming in the latter being twice as fast (0.26 versus 0.13 °C per decade) (Fig. 2). The velocity of climate change in the ocean (26.84 km per decade), as calculated from sea surface temperatures, was higher than in standing waters and over land, because of the smaller spatial temperature gradient (0.003 °C km^{-1}). The spatial temperature gradient in the ocean was a third of that in standing waters (0.009 °C km^{-1}) and nearly a sixth of that over land (0.017 °C km^{-1}). The velocity of climate change in the ocean is much less variable than in inland waters or on land (Fig. 2e), with small gradients punctuated by sharp thermal boundaries (for example, see the Gulf Stream). Areas of high velocity extend across larger regions in the ocean compared with the other ecosystems.

[1]Centre for Freshwater and Environmental Studies, Dundalk Institute of Technology, Dundalk, Ireland. [2]European Space Agency Climate Office, ECSAT, Didcot, UK. [3]UK Centre for Ecology & Hydrology, Lancaster Environment Centre, Lancaster, UK. ✉e-mail: riwoolway@gmail.com

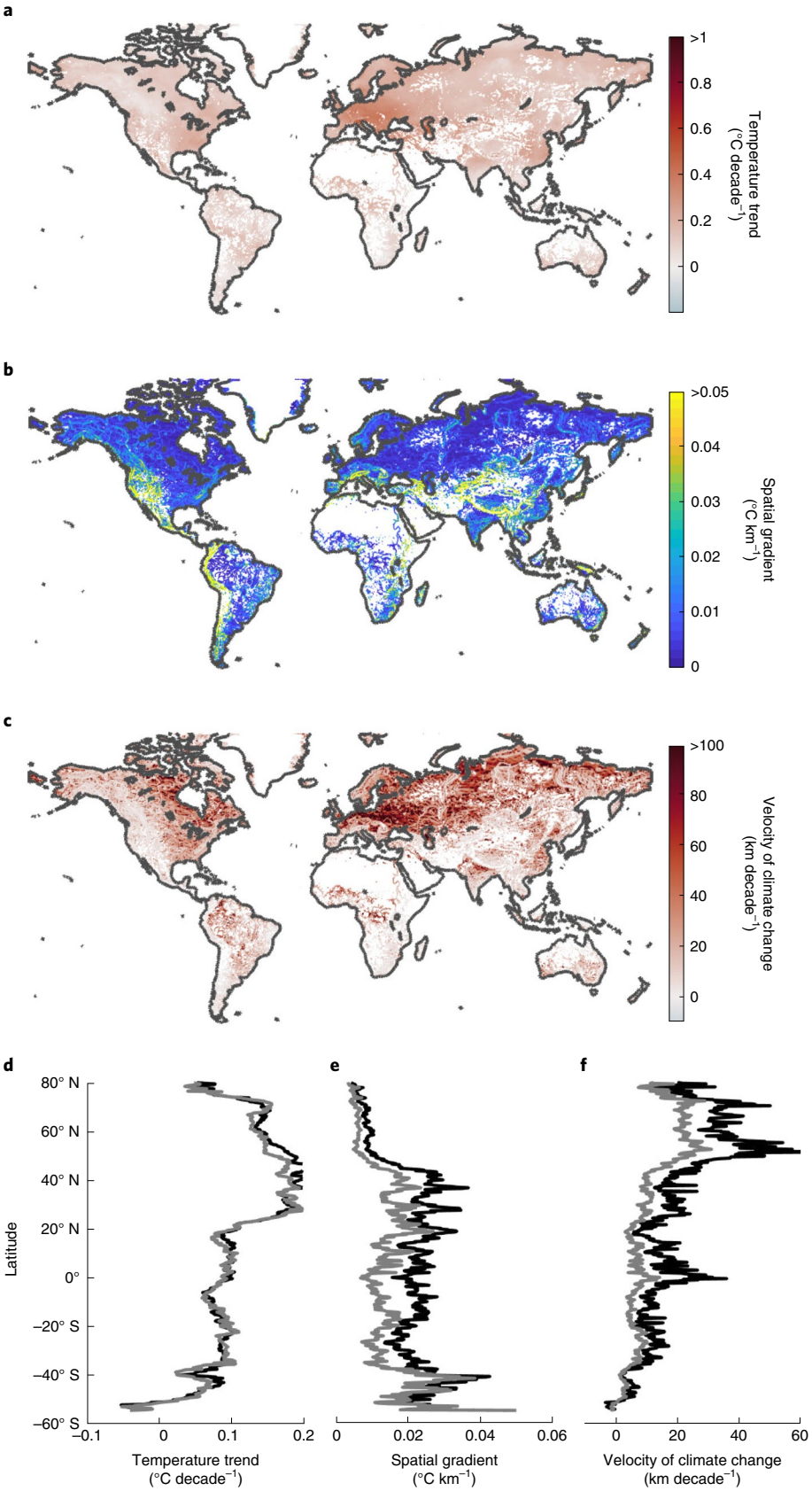

Fig. 1 | The velocity of climate change in the surface of standing waters (1979–2018). a, The annual surface water temperature trend (°C per decade). **b**, The two-dimensional spatial gradient of annual surface water temperature change (°C km^{-1}). **c**, The velocity of temperature change determined from the quotient of **a** and **b** (km per decade). **d**–**f**, The latitudinal mean (black) and median (grey) of the temperature trend (**d**), the spatial temperature gradient (**e**) and the velocity of climate change (**f**). White regions represent those where standing waters are absent from the global database.

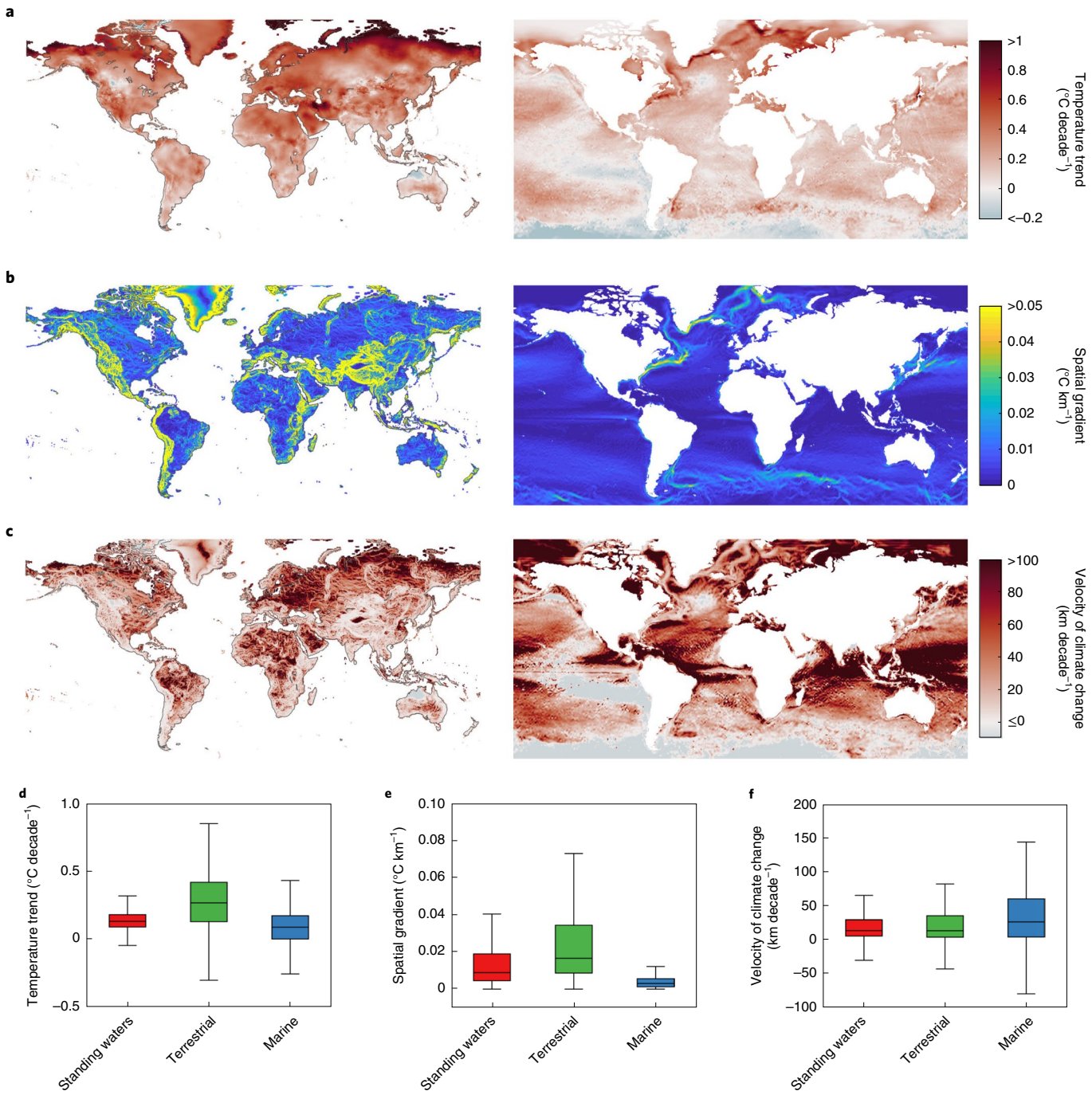

Fig. 2 | The velocity of climate change in terrestrial and marine ecosystems (1979–2018). a, The annual temperature trend (°C per decade) in terrestrial (left) and marine (right) ecosystems. **b**, The two-dimensional spatial gradient of annual surface temperature change (°C km^{-1}). **c**, The velocity of temperature change determined from the quotient of **a** and **b** (km per decade). **d**–**f**, Comparison of the surface temperature trend (**d**), spatial temperature gradient (**e**) and velocity of climate change (**f**) in standing waters with those calculated over land (terrestrial) and in the ocean (marine). Each box represents the interquartile range, the horizontal line is the median and the whiskers are 1.5× the interquartile range.

The climate velocities for inland standing waters calculated from ERA5 cannot be extended into the future, as the ERA5 temperatures are produced in near real time as an operational forecast. To project future changes in climate velocities, a different approach is required. Here we simulate the velocity of climate change during the twenty-first century using the same water temperature model as used in ERA5 during 1979–2018 (that is, FLake), but now force the model with bias-corrected climate projections from four global climate models: MIROC5, IPSL-CM5A-LR, GFDL-ESM2M and HadGEM2-ES (see Methods), on a 0.5° × 0.5° grid. These climate models contributed to phase 5 of the Coupled Model Intercomparison Project (CMIP5) and were bias-corrected within the Inter-Sectoral Impact Model Intercomparison Project (ISIMIP2b). Contemporary to future projections (2006–2099) for low, medium and high Representative Concentration Pathway (RCP) scenarios are investigated: RCP 2.6, 6.0 and 8.5, respectively (Fig. 3). For comparison, and to extend the record back in time, we also calculate the velocity of climate change from 1861 to

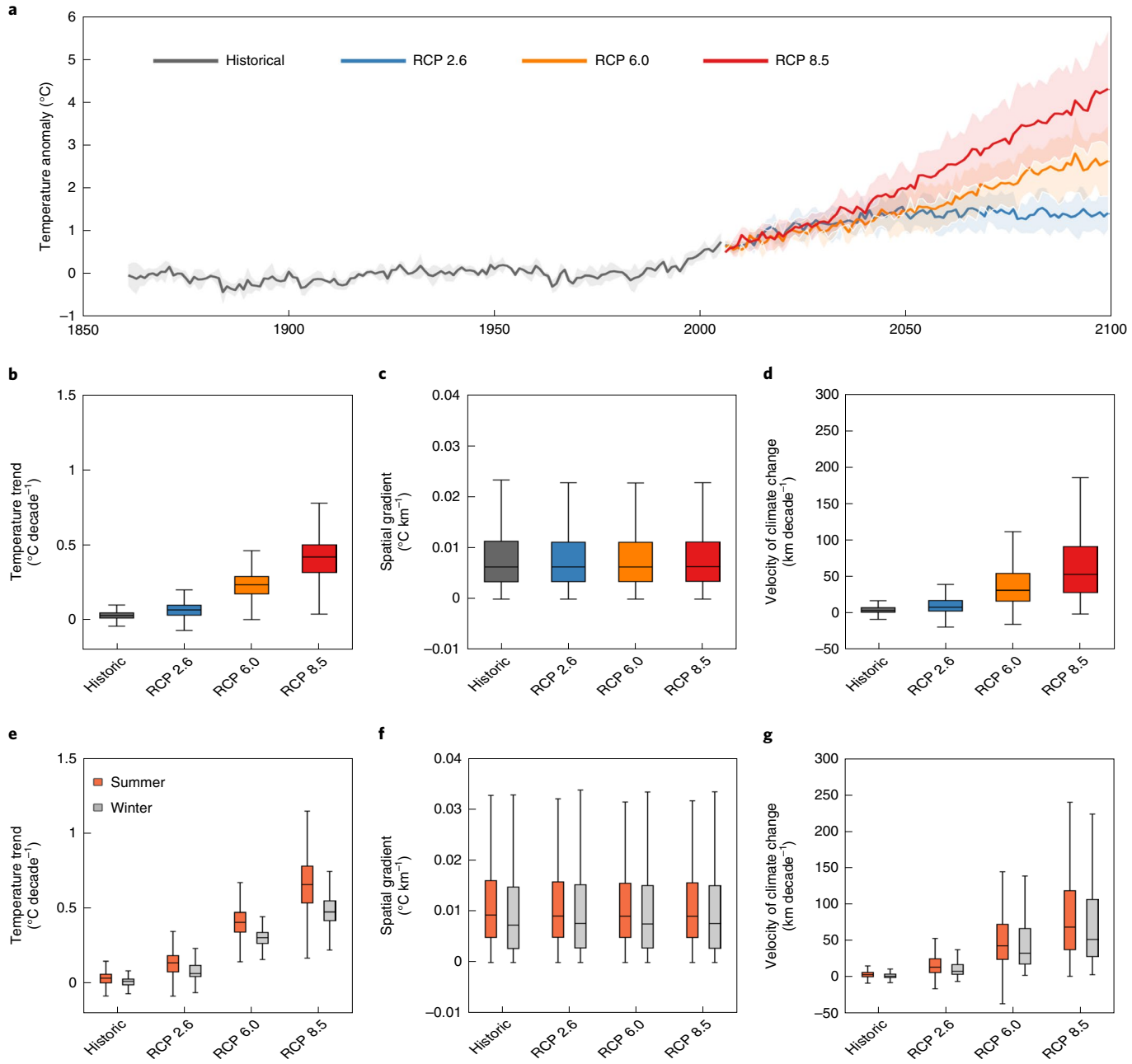

Fig. 3 | Historical and future projections of the velocity of climate change in inland standing waters. a, Temporal change in annual surface water temperature anomalies (relative to 1951–1980) from 1861 to 2099, showing the historical period (1861–2005) and contemporary to future climate projections (2006–2099) under three greenhouse gas concentration pathways (RCPs 2.6, 6.0 and 8.5). The thick lines show the average from the FLake model driven by four global climate models (MIROC5, IPSL-CM5A-LR, GFDL-ESM2M and HadGEM2-ES), and the shaded regions represent the standard deviation. **b**–**d**, Model projections of the temporal gradient of temperature change (°C per decade) (**b**), the two-dimensional spatial gradient of surface temperature change (°C km^{-1}) (**c**) and the velocity of climate change (km per decade) (**d**). **e**–**g**, Model projections for winter versus summer of the temporal gradient of temperature change (°C per decade) (**e**), the two-dimensional spatial gradient of surface temperature change (°C km^{-1}) (**f**) and the velocity of climate change (km per decade) (**g**). Each box represents the interquartile range, the horizontal line is the median and the whiskers are 1.5× the interquartile range. Each box contains the simulations from the FLake model forced by each of the climate model projections.

2005, where the historical climate simulations were forced using anthropogenic greenhouse gas and aerosol forcing in addition to natural forcing.

The magnitude of the surface air temperature change, which is one of the dominant drivers of surface warming in standing waters, increases considerably during the twenty-first century, with the magnitude of change increasing from RCP 2.6 to 6.0 to 8.5 (Extended Data Fig. 5). Our simulations demonstrate that the surface temperature of global standing waters will also increase during the twenty-first century (Fig. 3a). Specifically, under RCP 2.6, 6.0 and 8.5, surface water temperature trends will accelerate to 0.06 ± 0.04 °C per decade (quoted uncertainties represent the standard deviation from the FLake model driven by all four climate model projections), 0.23 ± 0.07 °C per decade and 0.40 ± 0.12 °C

per decade, respectively (Fig. 3b) from 2006 to 2099, compared with 0.03 ± 0.02 °C per decade from 1861 to 2005. Note that the temperature trend calculated from 1861 to 2005 is lower than that reported previously for the 1979–2018 period due to the rapid warming which occurred following the 1980s (Fig. 3a), in agreement with previous studies of observed lake surface temperature change[15]. The spatial gradient in temperature is similar across the different future climate scenarios (Fig. 3c), as well as the 1861–2005 period. Specifically, the spatial gradient was 0.0063 ± 0.00004 °C km^{-1} during the historical period, and marginally higher during the twenty-first century at 0.0064 ± 0.00005 °C km^{-1} under RCP 2.6 and 6.0, and 0.0065 ± 0.00009 °C km^{-1} under RCP 8.5. The model projections demonstrate that the median velocity of climate change from 1861 to 2005 was 3.5 ± 2.3 km per decade, again lower than in the 1979–2018 period due to the different temporal period considered. We project a median climate velocity during the period 2006–2099 of 8.7 ± 5.5 km per decade for RCP 2.6, 32.6 ± 10.3 km per decade for RCP 6.0 and 57.0 ± 17.0 km per decade for RCP 8.5.

The worldwide patterns of climate velocities are projected largely to hold under twenty-first century climate change, with areas that have experienced the highest velocities during the historical period (1861–2005) also typically experiencing the greatest velocities during the contemporary to future period (2006–2099). Specifically, there were statistically significant relationships between the worldwide climate velocities during the historical and future periods under RCP 2.6 ($R^2 = 0.52$; $P < 0.001$), RCP 6.0 ($R^2 = 0.48$; $P < 0.001$) and RCP 8.5 ($R^2 = 0.38$; $P < 0.001$), but with a decrease in correlation with an increase in the severity of climate change. There appear to be no systematic changes in the projected spatial patterns of climate velocity in the future; but some regions, such as Northern Europe, northeastern USA and northern Canada, will experience greater changes than others (Extended Data Fig. 6). The velocity of climate change in standing waters during the twenty-first century will be slightly greater in summer than in winter (Fig. 3e–g; summer was defined as July–September in the Northern Hemisphere and January–March in the Southern Hemisphere, with the opposite definition used for winter). For example, under RCP 8.5, our simulations suggest that, by the end of the current century, the median velocity of climate change will increase to 58.0 ± 13.2 km per decade during summer and 43.2 ± 10.5 km per decade during winter. This is a result of surface water temperatures in standing waters increasing at a faster rate in summer (0.59 ± 0.14 °C per decade) than in winter (0.47 ± 0.11 °C per decade), but is also influenced by a slightly higher median spatial temperature gradient in summer (0.008 ± 0.00007 °C km^{-1}) versus winter (0.007 ± 0.00007 °C km^{-1}) (Fig. 3).

The pace of climate change identified here for standing waters during the twenty-first century will produce new, and rapidly warming, thermal conditions for species at a given location. The ecological consequences will depend on the ability of a species to survive at a site, disperse within a catchment or disperse between catchments. The ability of a species to continue to survive at a site will depend on the temperature sensitivity of their most susceptible life-stages[16,17]. In addition, phenotypic plasticity may allow a species to acclimate to higher temperatures, while adaptation to higher temperatures is unlikely since rates of evolutionary change for critical thermal maxima are many orders of magnitude lower than even the rate of historical temperature trends[2,18]. In addition, cooler water at depth during seasonal stratification may provide a potential refuge from increasing surface water temperatures. However, the environment at depth may not always be suitable in terms of light, food supply or oxygen concentration. For example, some fish are unable to exploit cooler temperatures at depth because of low oxygen concentration[19], and oxygen depletion is likely to increase with climate change and continued eutrophication. Furthermore, the critical thermal period may occur in non-stratified periods of the year. For example, early life stages can be the most temperature sensitive[16], and these can occur in the winter when stratification is generally absent but the velocity of climate change is almost as great as in the summer. The evidence of summer fish-kills in lakes, and their lack of correlation with lake depth, suggests that depth may only provide a partial thermal refuge[4] and, as demonstrated in the oceans, climate velocities can be faster at depth than at the surface[20]. Phenological change in the response to warming may allow sensitive stages to exploit cooler times of the year, but where the seasonality of different components of the food web changes at different rates, the changing phenology could also cause food-web desynchronization, with potential negative consequences[21]. While there has been a focus on the consequence of rapid surface warming of inland standing waters for cold-water stenotherms at high latitudes[22], warm-water species that are close to their critical thermal limit at low latitudes are equally at risk[23].

Dispersal is an important life-history trait that, unlike the responses above, will not prevent species loss at a given site but may permit a species to survive by moving to cooler habitats. Within the dendritic hydrological network of a catchment, dispersal to cooler standing water can occur either upstream to higher elevations or, in large river systems, downstream to higher latitudes. However, species in headwaters or isolated tributaries may have a low connectivity to more suitable habitats and so be particularly susceptible to rapid warming[24]. For some species, such as freshwater molluscs, the rates of active dispersal of 1 to 10 km per decade (ref. [25]) are less than forecast future change under both medium and high greenhouse gas concentration pathways. While many amphibians move relatively small distances, at least some individuals may move over 10 km (ref. [26]). More motile species, such as some fish, have the potential to migrate rapidly in response to long-term climate change[10,27]. However, in all cases, dispersal may be limited by physical and ecological barriers caused by the complex mosaic of freshwater environments. The increasing number of dams on the world's rivers[28] may further restrict dispersal by preventing access to upstream reaches and because the habitat in the intervening reservoir may be unsuitable. Even greater challenges are faced in dispersal across land to cooler catchments at higher elevation or higher latitude, as illustrated by the fragmented distribution of fish within a landscape[29] and the high degree of endemism in freshwater organisms[30]. Aquatic insects have a variable potential to disperse actively between catchments in their adult stage[31], while other organisms depend on vectors such as wind or transport by large motile animals such as birds[32]. For dispersal within and between catchments, colonization and expansion in cooler areas may be impeded by interactions with the resident community of species that can restrict the establishment of new species despite an adequate propagule pressure[32].

The discussion above outlines the challenges that species in inland waters face in responding to rapid climate change. Although the velocity of climate change of inland standing waters is about half that of the ocean, the future consequences for the conservation of species, and the goods and services they provide, are likely to be much greater. This is caused by the combination of low dispersal rates of some freshwater species, substantial barriers to dispersal and ongoing major disruption to inland water biodiversity and ecosystem function by multiple anthropogenic stressors[30]. A recent analysis showed that the tracking of isothermal shifts in latitude in terrestrial species was six times slower than in marine species[33]; this tracking is likely to be even slower for species from inland standing waters. Placing this global analysis in a conservation context will require information on the thermal tolerance of different freshwater species, their dispersal ability and the local and regional connectivity of their habitat. It will also require the more complex interactions between species within a community to be understood and, for species such as amphibians and some insects and fish with life stages in different environments, the consequences of environmental change experienced in different realms.

Online content

Any methods, additional references, Nature Research reporting summaries, source data, extended data, supplementary information, acknowledgements, peer review information; details of author contributions and competing interests; and statements of data and code availability are available at https://doi.org/10.1038/s41558-020-0889-7.

Received: 10 October 2019; Accepted: 30 July 2020;
Published online: 21 September 2020

References

1. Costanza, R. et al. The value of the world's ecosystem services and natural capital. *Nature* **387**, 253–260 (1997).
2. O'Reilly, C. et al. Rapid and highly variable warming of lake surface waters around the globe. *Geophys. Res. Lett.* **42**, 10773–10781 (2015).
3. Woolway, R. I. & Merchant, C. J. Worldwide alteration of lake mixing regimes in response to climate change. *Nat. Geosci.* **12**, 271–276 (2019).
4. Till, A. et al. Fish die-offs are concurrent with thermal extremes in north temperate lakes. *Nat. Clim. Change* **9**, 637–641 (2019).
5. Abell, R. et al. Freshwater ecoregions of the world: a new map of biogeographic units for freshwater biodiversity conservation. *BioScience* **58**, 403–414 (2008).
6. Maberly, S. C. et al. Global lake thermal regions shift under climate change. *Nat. Commun.* **11**, 1232 (2020).
7. Woolway, R. I. & Merchant, C. J. Intralake heterogeneity of thermal responses to climate change: a study of large Northern Hemisphere lakes. *J. Geophys. Res. Atmos.* **123**, 3087–3098 (2018).
8. Winslow, L. A. et al. Small lakes show muted climate change signal in deepwater temperatures. *Geophys. Res. Lett.* **42**, 355–361 (2015).
9. Winslow, L. A. et al. Seasonality of change: summer warming rates do not fully represent effects of climate change on lake temperatures. *Limnol. Oceanogr.* **62**, 2168–2178 (2017).
10. Comte, L. & Grenouillet, G. Do stream fish track climate change? Assessing distribution shifts in recent decades. *Ecography* **36**, 1236–1246 (2013).
11. Loarie, S. R. et al. The velocity of climate change. *Nature* **462**, 1052–1055 (2009).
12. Burrows, M. T. et al. The pace of shifting climate in marine and terrestrial ecosystems. *Science* **334**, 652–655 (2011).
13. Burrows, M. T. et al. Geographical limits to species-range shifts are suggested by climate velocity. *Nature* **507**, 492–495 (2014).
14. Woodward, G. et al. Climate change and freshwater ecosystems: impacts across multiple levels of organization. *Philos. Trans. R. Soc. B* **365**, 2093–2106 (2010).
15. Woolway, R. I. et al. Warming of Central European lakes and their response to the 1980s climate regime shift. *Climatic Change* **142**, 505–520 (2017).
16. Realis-Doyelle, E. et al. Strong effects of temperature on the early life stages of a cold stenothermal fish species, brown trout (*Salmo trutta* L.). *PLoS ONE* **11**, e0155487 (2016).
17. Dahlke, F. T., Wohlrab, S., Butzin, M. & Pörtner, H. Thermal bottlenecks in the life cycle define climate vulnerability of fish. *Science* **369**, 65–70 (2020).
18. Comte, L. & Olden, J. D. Climatic vulnerability of the world's freshwater and marine fishes. *Nat. Clim. Change* **7**, 718–722 (2017).
19. Jones, I. D. et al. Assessment of long-term changes in habitat availability for Arctic charr (*Salvelinus alpinus*) in a temperate lake using oxygen profiles and hydroacoustic surveys. *Freshw. Biol.* **53**, 393–402 (2008).
20. Brito-Morales, I. et al. Climate velocity reveals increasing exposure of deep-ocean biodiversity to future warming. *Nat. Clim. Change* **10**, 576–581 (2020).
21. Thackeray, S. J. et al. Food web de-synchronization in England's largest lake: an assessment based on multiple phenological metrics. *Glob. Change Biol.* **19**, 3568–3580 (2013).
22. Walters, A. W. et al. The interaction of exposure and warming tolerance determines fish species vulnerability to warming stream temperatures. *Biol. Lett.* **14**, 2018342 (2018).
23. Duarte, H. et al. Can amphibians take the heat? Vulnerability to climate warming in subtropical and temperate larval amphibian communities. *Glob. Change Biol.* **18**, 412–421 (2012).
24. Rader, R. B., Unmack, P. J., Christensen, W. F. & Jiang, X. Connectivity of two species with contrasting dispersal abilities: a test of the isolated tributary hypothesis. *Freshw. Sci.* **38**, 142–155 (2019).
25. Kappes, H. & Haase, P. Slow, but steady: dispersal of freshwater molluscs. *Aquat. Sci.* **74**, 1–14 (2012).
26. Smith, M. A. & Green, D. M. Dispersal and the metapopulation paradigm in amphibian ecology and conservation: are all amphibian populations metapopulations? *Ecography* **28**, 110–128 (2005).
27. Comte, L. & Olden, J. D. Fish dispersal in flowing waters: a synthesis of movement- and genetic-based studies. *Fish Fish.* **19**, 1063–1077 (2018).
28. Zarfl, C. et al. A global boom in hydropower dam construction. *Aquat. Sci.* **7**, 1279–1299 (2015).
29. Carvajal-Quintero, J. et al. Drainage network position and historical connectivity explain global patterns in freshwater fishes' range size. *Proc. Natl Acad. Sci. USA* **116**, 13434–13439 (2019).
30. Strayer, D. L. & Dudgeon, D. Freshwater biodiversity conservation: recent progress and future challenges. *J. N. Am. Benthol. Soc.* **29**, 344–358 (2010).
31. Hughes, J. M. et al. Genes in streams: using DNA to understand the movement of freshwater fauna and their riverine habitat. *BioScience* **59**, 573–583 (2009).
32. Incagnone, G. et al. How do freshwater organisms cross the 'dry ocean'? A review on passive dispersal and colonization process with a special focus on temporary ponds. *Hydrobiologia* **750**, 103–123 (2015).
33. Lenoir, J. et al. Species better track climate warming in the oceans than on land. *Nat. Ecol. Evol.* **4**, 1044–1059 (2020).

Methods

Temperature data. Water temperatures from 1979 to 2018 were downloaded from the ECMWF ERA5 re-analysis product at a grid resolution of 0.25° × 0.25°. The surface water temperature of global standing waters was simulated within ERA5 (ref. [34]) via the FLake model[35,36], which is implemented within HTESSEL[37,38] of the ECMWF Integrated Forecasting System (IFS). The water temperature model is one of the most widely used lake models and has been tested extensively in past studies[3,39]. The lake surface temperatures from ERA5 were also validated here with satellite-derived lake surface temperatures from the European Space Agency (ESA) Climate Change Initiative (CCI) Lakes project (CCI Lakes; http://cci.esa.int/lakes) that provides, among other things, daily observations of lake surface temperature at a grid resolution of 1/120° for 250 lakes worldwide. From version 1.0 of the CCI Lakes dataset[40], we selected only lakes based on the existence of a 10 × 10 pixel array of pure water surrounding the lake centre, following the recommendations of ref. [41]. For each of these lakes, a 3 × 3 pixel array was then extracted for each day, and the average of these pixels was then calculated before comparison with the ERA5 data, which were also extracted for the lake-centre location. The satellite-derived lake temperatures used in the study were acquired between 2007 and 2018, the period during which most satellite retrievals were available in ESA CCI Lakes. Good agreement was obtained between the simulations and satellite-derived observations of lake surface temperature (Extended Data Fig. 1). A detailed description of the surface temperature model and the implementation of surface water temperature in the IFS is provided in ref. [42]. The surface water temperature model in the IFS is supported by two climatological fields: (i) an inland water mask, provided by the US Department of Agriculture–Global Land Cover Characteristics data[43], at a nominal resolution of 1 km, which provides the fractions of each surface grid occupied by surface water; (ii) depth, which is specified according to ref. [44] and combined with a global bathymetry dataset, ETOPO1, which is a 1 arcmin global relief model of the Earth's surface that integrates land topography and ocean bathymetry. Surface air temperature over land and sea surface temperatures were also downloaded by ERA5 from 1979 to 2018 at a grid resolution of 0.25° × 0.25°. All data from January 1979 to December 2018, inclusive, were accessed and analysed at an hourly resolution. Annual and seasonal averages, which were used in all velocity calculations, were then calculated from the hourly data. Summer and winter temperatures were calculated for standing waters. Following ref. [2], summer was defined as 1 July to 30 September for lakes situated in the Northern Hemisphere and from 1 January to 31 March in the Southern Hemisphere.

Climate model projections. To calculate the velocity of climate change during the twenty-first century, we used the same water temperature model as in ERA5 but driven by bias-corrected climate projections from four climate models (GFDL-ESM2M, HadGEM2-ES, IPSL-CM5A-LR and MIROC5) for historical (1861–2005) and contemporary to future periods (2006–2099) under three scenarios: RCP 2.6, 6.0 and 8.5. Similar to ref. [3], we downloaded atmospheric forcing data (air temperature at 2 m, wind speed at 10 m, surface solar and thermal radiation and specific humidity) needed to drive FLake from ISIMIP2b (https://www.isimip.org/protocol/#isimip2b). All climate projection data were available at daily intervals and at a grid resolution of 0.5°. These data were used as inputs to the model after bias adjustment to the EWEMBI reference dataset[45,46]. To drive the surface water temperature model, lake depths were determined from the Global Lakes and Wetlands Database[47], aggregated from the original 30-arcsec Global Lake Data Base[44,48,49] to a 0.5° × 0.5° grid lake depth field. The depth dataset used by the lake model (that is, the average depth of all lakes within a grid) could influence the future projections, given that depth is an important lake attribute that influences the thermal response of lakes to climate change[3,50]. Notably, lakes of different depths within a grid could behave differently than those included here, which is a limitation that should be considered when interpreting these results.

Velocity of climate change. Climate velocities (km per year) were calculated by dividing long-term temperature trends (°C per decade) by the spatial temperature gradient (°C km^{-1}). Long-term trends of each grid cell were calculated as the slope of a linear trend model, and the spatial gradients were calculated using a 3 × 3 grid cell neighbourhood. Finally, the spatial temperature gradient was calculated as the vector sum of the north–south and east–west temperature gradients. Specifically, the spatial temperature gradient for a focal cell was calculated as the difference in temperature for each northern and southern pair divided by the distance between them[12]. For these calculations we used the *R* package 'Vocc' (refs. [51,52]).

Reporting Summary. Further information on research design is available in the Nature Research Reporting Summary linked to this article.

Data availability

ERA5 data used in this study are available from https://cds.climate.copernicus.eu/cdsapp#!/dataset/reanalysis-era5-single-levels?tab=overview. The FLake model source code is available to download from http://www.flake.igb-berlin.de/. Climate model projections are available at https://www.isimip.org/protocol/#isimip2b.

References

34. Hersbach, H. et al. The ERA5 Global Reanalysis. *Q. J. R. Meteorol. Soc.* https://doi.org/10.1002/qj.3803 (2020).
35. Mironov, D. *Parameterization of Lakes in Numerical Weather Prediction. Part 1: Description of a Lake Model* COSMO Technical Report No. 11 (Deutscher Wetterdienst, 2008).
36. Mironov, D. et al. Implementation of the lake parameterisation scheme FLake into the numerical weather prediction model COSMO. *Boreal Environ. Res.* **15**, 218–230 (2010).
37. Dutra, E. et al. An offline study of the impact of lakes on the performance of the ECMWF surface scheme. *Boreal Environ. Res.* **15**, 100–112 (2010).
38. Balsamo, G. et al. On the contribution of lakes in predicting near-surface temperature in a global weather forecasting model. *Tellus A* **64**, 15829 (2012).
39. Le Moigne, P., Colin, J. & Decharme, B. Impact of lake surface temperatures simulated by the FLake scheme in the CNRM-CM5 climate model. *Tellus A* **68**, 31274 (2016).
40. Crétaux, J.-F., et al. ESA Lakes Climate Change Initiative (Lakes_cci): lake products, version 1.0. *Centre for Environmental Data Analysis* https://doi.org/10.5285/3c324bb4ee394d0d876fe2e1db217378 (2020).
41. Schneider, P. & Hook, S. J. Space observations of inland water bodies show rapid surface warming since 1985. *Geophys. Res. Lett.* **37**, L22405 (2010).
42. IFS documentation CY45R1, part IV: physical processes *ECMWF* https://www.ecmwf.int/node/18714 (2018).
43. Loveland, T. R. et al. Development of a global land cover characteristics database and IGBP DISCover from 1km AVHRR data. *Int. J. Remote Sens.* **21**, 1303–1330 (2000).
44. Kourzeneva, E. External data for lake parameterization in numerical weather prediction and climate modelling. *Boreal Environ. Res.* **15**, 165–177 (2010).
45. Frieler, K. et al. Assessing the impacts of 1.5 °C global warming–simulation protocol of the inter-sectoral impact model intercomparison project (ISIMIP2b). *Geosci. Model Dev.* **10**, 4321–4345 (2017).
46. Lange, S. EartH2Observe, WFDEI and ERA-interim data merged and bias-corrected for ISIMIP (EWEMBI). V.1.1. *GFZ Data Services* https://doi.org/10.5880/pik.2019.004 (2019).
47. Lehner, B. & Döll, P. Development and validation of a global database of lakes, reservoirs and wetlands. *J. Hydrol.* **296**, 1–22 (2004).
48. Subin, Z. M., Riley, W. J. & Mironov, D. An improved lake model for climate simulations: Model structure, evaluation, and sensitivity analyses in CESM1. *J. Adv. Model. Earth Syst.* **4**, M02001 (2012).
49. Choulga, M., Kourzeneva, E., Zakharova, E. & Doganovsky, A. Estimation of the mean depth of boreal lakes for use in numerical weather prediction and climate modelling. *Tellus A* **66**, 21295 (2014).
50. Woolway, R. I. & Merchant, C. J. Amplified surface temperature response of cold, deep lakes to inter-annual air temperature variability. *Sci. Rep.* **7**, 4130 (2017).
51. R Development Core Team R: a language and environment for statistical computing, *R Foundation for Statistical Computing* http://www.R-project.org/ (2018).
52. Molinos, J. G. et al. VoCC: an R package for calculating the velocity of climate change and related climatic metrics. *Methods Ecol. Evol.* **10**, 2195–2202 (2019).

Acknowledgements

R.I.W. received funding from the European Union's Horizon 2020 research and innovation programme under Marie Skłodowska-Curie grant agreement no. 791812. S.C.M. was funded by the NERC Hydroscape Project (NE/N00597X/1).

Author contributions

Both authors developed the concept of the study. R.I.W. performed the modelling. S.C.M. and R.I.W. led the drafting of the manuscript, and both approved the final version of the manuscript.

Competing interests

The authors declare no competing interests.

Additional information

Extended data is available for this paper at https://doi.org/10.1038/s41558-020-0889-7.

Supplementary information is available for this paper at https://doi.org/10.1038/s41558-020-0889-7.

Correspondence and requests for materials should be addressed to R.I.W.

Peer review information *Nature Climate Change* thanks Lise Comte and the other, anonymous, reviewer(s) for their contribution to the peer review of this work.

Reprints and permissions information is available at www.nature.com/reprints.

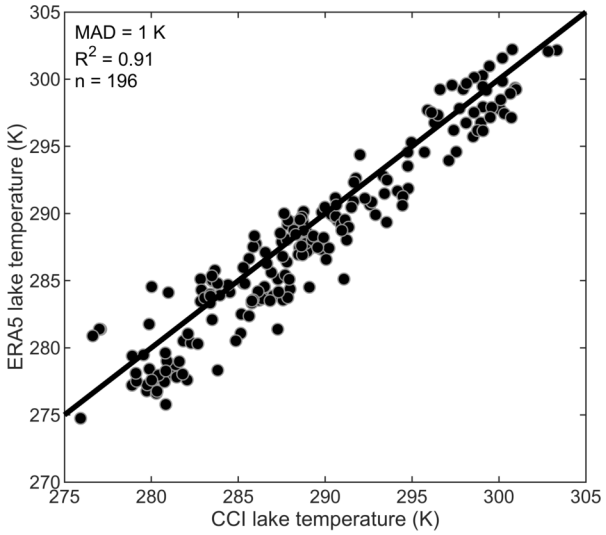

Extended Data Fig. 1 | Validation of simulated lake surface temperatures. Comparison of simulated and satellite-derived surface water temperatures for 196 lakes (2007-2018) from the ESA CCI Lakes dataset. Shown are comparisons of the average open-water temperatures for the lake-centre pixels.

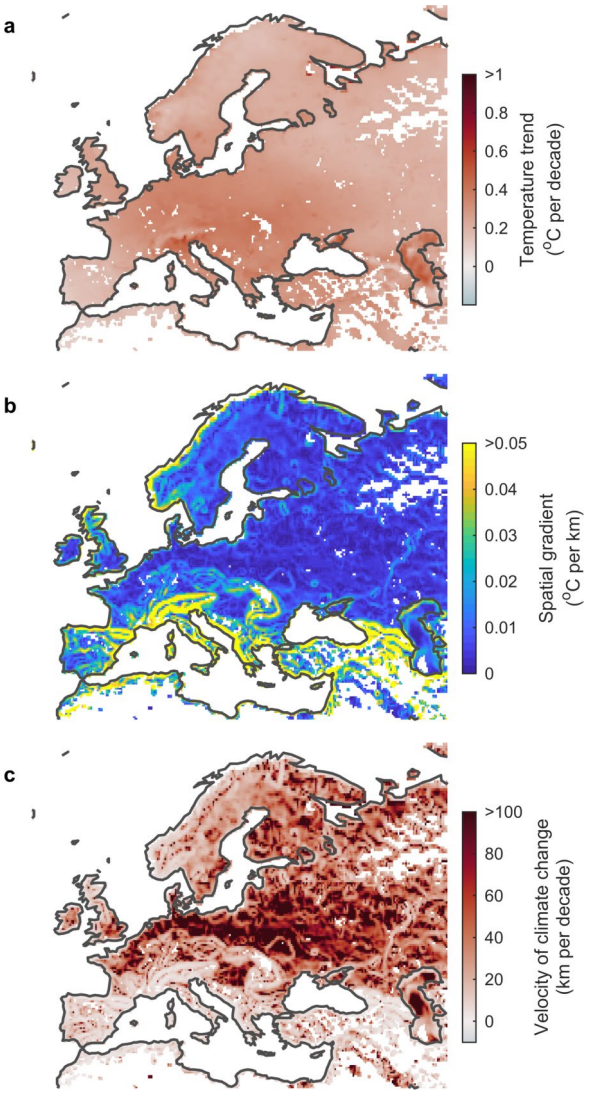

Extended Data Fig. 2 | The velocity of climate change in European standing waters. Shown for standing waters in Europe are **a**, the surface water temperature trend, **b**, the two-dimensional spatial gradient of surface water temperature change, and **c**, the velocity of climate change during the 1979 to 2018 period. White regions represent those where standing waters are absent within the global database.

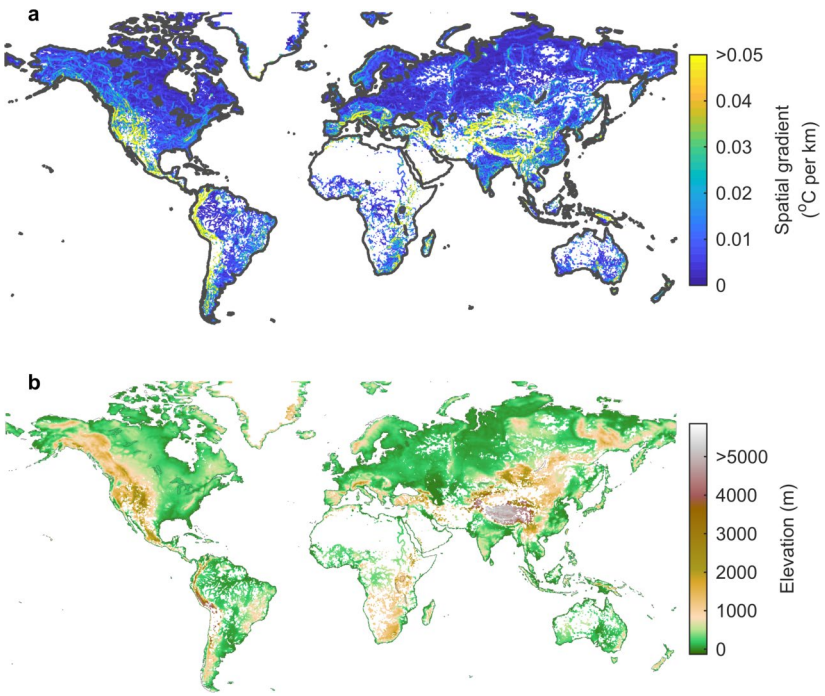

Extended Data Fig. 3 | Global relationship between the spatial temperature gradient and elevation. Shown is a comparison of **a**, the two-dimensional spatial gradient of surface water temperature change, and **b**, elevation. White regions represent those where standing waters are absent within the global database.

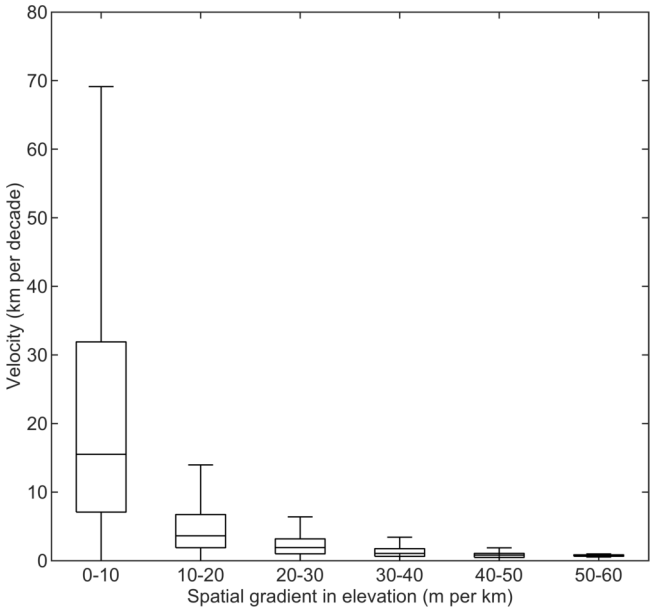

Extended Data Fig. 4 | Comparison of the velocity of climate change and the spatial elevation gradient. Shown is the relationship between the velocity of climate change in the surface of inland surface waters and the two-dimensional spatial gradient of elevation change. Specifically, we show that climate change velocities are greater at sites with low elevation gradients. Thus, steep sites which show rapid change in elevation, experience lower climate velocities. Each box represents the interquartile range, the horizontal line is the median, and the whiskers are 1.5 times the interquartile range.

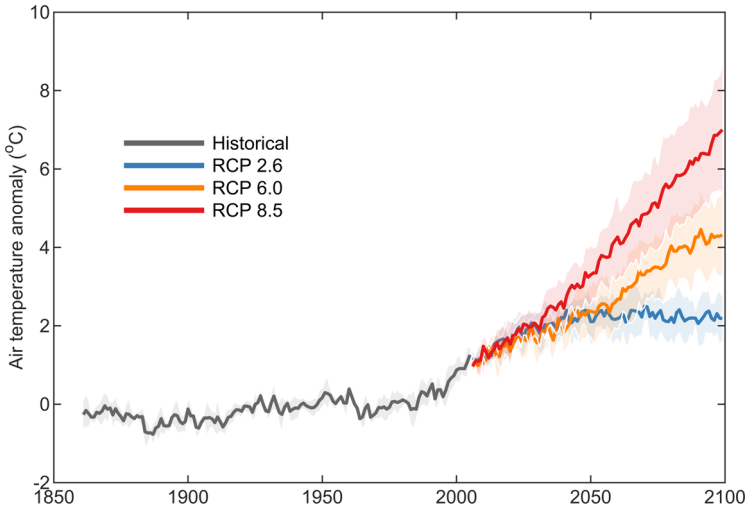

Extended Data Fig. 5 | Historic and future projections of global surface air temperature. Temporal change in annual surface air temperature anomalies (relative to 1951-1980) from 1861-2099 showing the historic period (1861-2005), with contemporary to future climate projections (2006-2099) under three representative greenhouse gas concentration scenarios (RCPs 2.6, 6.0, 8.5). The thick lines show the average of four global climate models (MIROC5, IPSL-CM5A-LR, GFDL-ESM2M, HadGEM2-ES), and the shaded regions represent the standard deviation.

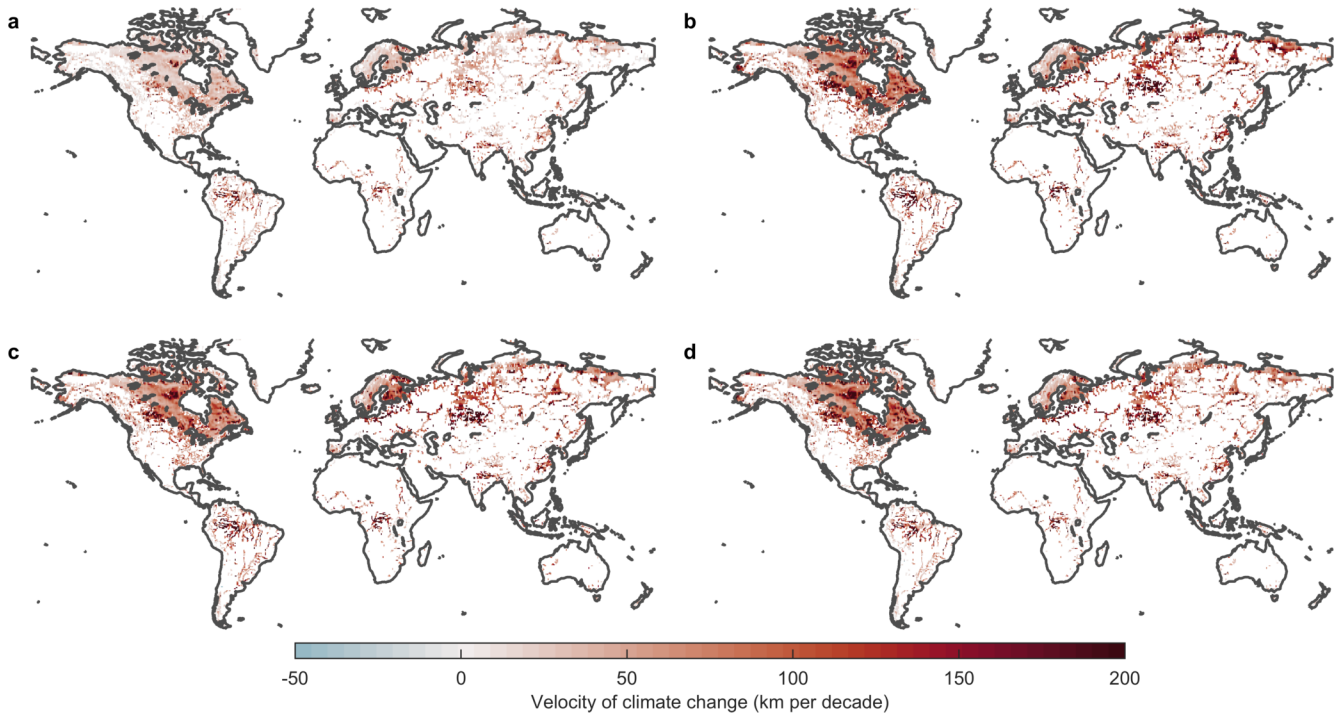

Extended Data Fig. 6 | Global variations in the velocity of climate change from 2006-2099 relative to 1861-2005. Shown are the differences in the simulated velocity of climate change between the historic (1861-2005) and the contemporary to future (2006-2099) period (that is, future minus historic) under RCP 8.5. Results are shown for the lake model forced by four global climate models (a, MIROC5; b, IPSL-CM5A-LR; c, GFDL-ESM2M; d, HadGEM2-ES). White regions represent those where the difference in climate velocities are negligible.

nature research

Corresponding author(s): R. Iestyn Woolway

Last updated by author(s): Jul 15, 2020

Reporting Summary

Nature Research wishes to improve the reproducibility of the work that we publish. This form provides structure for consistency and transparency in reporting. For further information on Nature Research policies, see Authors & Referees and the Editorial Policy Checklist.

Statistics

For all statistical analyses, confirm that the following items are present in the figure legend, table legend, main text, or Methods section.

n/a	Confirmed	
☐	☒	The exact sample size (*n*) for each experimental group/condition, given as a discrete number and unit of measurement
☒	☐	A statement on whether measurements were taken from distinct samples or whether the same sample was measured repeatedly
☒	☐	The statistical test(s) used AND whether they are one- or two-sided *Only common tests should be described solely by name; describe more complex techniques in the Methods section.*
☒	☐	A description of all covariates tested
☒	☐	A description of any assumptions or corrections, such as tests of normality and adjustment for multiple comparisons
☐	☒	A full description of the statistical parameters including central tendency (e.g. means) or other basic estimates (e.g. regression coefficient) AND variation (e.g. standard deviation) or associated estimates of uncertainty (e.g. confidence intervals)
☒	☐	For null hypothesis testing, the test statistic (e.g. *F*, *t*, *r*) with confidence intervals, effect sizes, degrees of freedom and *P* value noted *Give P values as exact values whenever suitable.*
☒	☐	For Bayesian analysis, information on the choice of priors and Markov chain Monte Carlo settings
☒	☐	For hierarchical and complex designs, identification of the appropriate level for tests and full reporting of outcomes
☒	☐	Estimates of effect sizes (e.g. Cohen's *d*, Pearson's *r*), indicating how they were calculated

Our web collection on statistics for biologists contains articles on many of the points above.

Software and code

Policy information about availability of computer code

Data collection	ERA5 data used in this study are available from https://cds.climate.copernicus.eu/#!/home
Data analysis	We used R version 3.5.2. No custom algorithms or software were used.

For manuscripts utilizing custom algorithms or software that are central to the research but not yet described in published literature, software must be made available to editors/reviewers. We strongly encourage code deposition in a community repository (e.g. GitHub). See the Nature Research guidelines for submitting code & software for further information.

Data

Policy information about availability of data

All manuscripts must include a data availability statement. This statement should provide the following information, where applicable:

- Accession codes, unique identifiers, or web links for publicly available datasets
- A list of figures that have associated raw data
- A description of any restrictions on data availability

ERA5 data used in this study are available from https://cds.climate.copernicus.eu/#!/home. The lake model source code is available to download from http://www.flake.igb-berlin.de/. Climate model projections are available at https://www.isimip.org/protocol/#isimip2b.

Field-specific reporting

Please select the one below that is the best fit for your research. If you are not sure, read the appropriate sections before making your selection.

☐ Life sciences ☐ Behavioural & social sciences ☒ Ecological, evolutionary & environmental sciences

Ecological, evolutionary & environmental sciences study design

All studies must disclose on these points even when the disclosure is negative.

Study description	In this study, we calculate the velocity of climate change as the quotient of the long-term temperature trend to the two-dimensional spatial gradient in temperature.
Research sample	We calculated the distribution of the velocity of climate change using surface water temperatures from a new state-of-the-art global reanalysis from the European Centre for Medium-Range Weather Forecasts (ECMWF), ERA5, on a 0.25°-by-0.25° grid. Also, we used the FLake model forced with bias-corrected climate projections from an ensemble of climate model projections from ISIMIP2b.
Sampling strategy	We used the highest spatial resolution temperature data available for the historic period (i.e., ERA5) and used the most commonly used lake model for the future simulations.
Data collection	Modelled temperatures were used in this study
Timing and spatial scale	Historic period: Jan 1979 to Dec 2018 at hourly resolution. Climate change scenarios: Jan 1861 to Dec 2099 at daily resolution.
Data exclusions	No data were excluded from the analysis
Reproducibility	All data is openly available
Randomization	Not relevant as all temperature simulations were used
Blinding	All temperature simulations were analysed

Did the study involve field work? ☐ Yes ☒ No

Reporting for specific materials, systems and methods

We require information from authors about some types of materials, experimental systems and methods used in many studies. Here, indicate whether each material, system or method listed is relevant to your study. If you are not sure if a list item applies to your research, read the appropriate section before selecting a response.

Materials & experimental systems

n/a	Involved in the study
☒	☐ Antibodies
☒	☐ Eukaryotic cell lines
☐	☐ Palaeontology
☒	☐ Animals and other organisms
☒	☐ Human research participants
☒	☐ Clinical data

Methods

n/a	Involved in the study
☒	☐ ChIP-seq
☒	☐ Flow cytometry
☒	☐ MRI-based neuroimaging

Palaeontology

Specimen provenance	NA
Specimen deposition	NA
Dating methods	NA

☐ Tick this box to confirm that the raw and calibrated dates are available in the paper or in Supplementary Information.